124 | https://doi.org/10.3311/PPch.12291
Creative Commons Attribution

Periodica Polytechnica Chemical Engineering, 64(1), pp. 124–134, 2020

Investigating the Advantages and Limitations of Modeling Physical Mass Transfer of CO_2 on Flat Plate by One Fluid Formulation in OpenFOAM

Phanindra Prasad Thummala[1*], Umran Tezcan Un[2], Ahmet Ozan Celik[3]

[1] Graduate School of Science, Anadolu University, 26555 Eskisehir, Turkey
[2] Department of Environmental Engineering, Anadolu University, 26555 Eskisehir, Turkey
[3] Department of Civil Engineering, Anadolu University, 26555 Eskisehir, Turkey
* Corresponding author, e-mail: phanindrapt@anadolu.edu.tr

Received: 23 March 2018, Accepted: 25 July 2018, Published online: 07 January 2019

Abstract

One fluid formulation is an approach used for modeling and analysis of mass transfer between two immiscible phases. In this study we implement and analyze the advantages and limitations of this approach for CO_2 physical mass transfer into MEA. The domain is a flat plate and gas liquid flow is counter current. The analysis was carried for operating parameters like liquid phase Reynolds number, MEA mass fraction and the angle of inclination of flat plate. The results clearly show that the model effectively captures the deviation in liquid side mass transfer coefficient due to the surface instabilities and liquid properties which are generally neglected by standard correlations. Also the model shows that the standard Higbie correlation is preferable at low Reynolds number at any angle of inclination. The grid independent studies show that a size of 6.25 μm is required in the interface region for effectively using this approach. The computational resource time at this resolution was found as the only limitation for using this approach and we suggest a procedure to overcome this limitation. The present simulation results can help CFD researchers investigating immiscible gas-liquid mass transfer using OpenFOAM.

Keywords

one fluid formulation, CO_2 absorption, liquid mass transfer coefficient, OpenFOAM

1 Introduction

CO_2 is the main greenhouse gas that is causing an increase in average surface temperature of earth and need to be captured at the source to reduce its impact on the environment. The main sources of CO_2 emission are power plants, industrial processes and domestic consumption of fuels. Nearly 40 % of this total CO_2 emission originates from industries [1]. Hence, technologies required to capture the CO_2 gas at the source need to be developed. Several technologies have been developed in this regard like membrane separations (utilizing a membrane to separate the CO_2 from flue gases) [2], adsorption (adsorbing the CO_2 on the surface of the chemically activated solids) [3] and using solvents like ionic liquids [4], amines blends [5] (with and without reactions). Among all of them the absorption of CO_2 by MEA (*mono ethyl amine*) solvent is one of the most preferred technique [6]. CO_2 absorption into MEA is majorly carried using packed bed reactors. Various kinds of reactors like bubble column, stirred tank, packed bed reactors, fluidized bed reactor, membrane reactors and hybrid reactors combining above reactor types [7] are available for effective utilization of absorption phenomena. Among them, the availability of high interfacial area for mass transfer at low pressure drop makes the packed bed reactors preferable, commercially tested at industrial scale [8], for gas liquid absorption process.

The packed bed reactors facilitate high interfacial areas using either structured packings or random packings. Structured packings are found to give higher mass transfer rates [9–12]. The efficiency of a structured packing depends majorly upon micro level interactions between gas liquid immiscible phases next to packing surface. Hence understanding the microlevel mass transfer helps in developing better design and effective utilization of packed bed reactors [13, 14].

Computational fluid dynamics (CFD) is an effective tool in understanding the dynamics of multi-phase flows

Cite this article as: Prasad Thummala, P., Tezcan Un, U., Celik, A. O. "Investigating the Advantages and Limitations of Modeling Physical Mass Transfer of CO_2 on Flat Plate by One Fluid Formulation in OpenFOAM", Periodica Polytechnica Chemical Engineering, 64(1), pp. 124–134, 2020. https://doi.org/10.3311/PPch.12291

in complex geometries. CFD reduces the overall number of experiments and allow access to velocity, temperature and other scalar and vector fields of interest at any location of the geometry, which otherwise is very difficult to be accessed by experimental techniques [15]. A detailed overview of utilizing CFD as an effective tool in modeling absorption in packed bed can be found the recent article published by Haroun and Raynal [16].

The micro level analysis of structured packing essentially involves modeling of multiphase fluid dynamics as immiscible phase flow where the fluids are not interpenetrating. The immiscible two phase flow is generally modeled using Volume of Fluid (VOF) approach and results are comparable to experimental values derived using particle image velocimetry techniques [17]. The mass transfer across these immiscible fluids is modeled majorly in two different ways. One approach involves the modeling of mass transfer across the immiscible phases by explicitly adding source terms to the governing equations of VOF approach. Sebastia-Saez et al. [15, 18, 19] modeled physical and reactive mass transfer on flat and texture plates by this approach. The geometry in their work was same as that of Hoffmann et al. [17]. A similar approach was used by Xu et al. [20] for modeling the mass transfer of propane gas into toluene liquid.

Another approach for modeling the mass transfer across immiscible phases is familiarly known as "one fluid approach" or "continuous specie transfer (CST)" approach. This approach was proposed and validated by Haroun et al. [21]. The model has an advantage of avoiding any kind of assumptions in terms of input parameters like mass transfer coefficient values derived from standard correlations. This model was also used in detailed numerical simulation of (direct numerical simulation, DNS) structured packing sheet also to derive mass transfer and liquid hold up in structured packing element by same group. The group of Haroun used JADIM multiphase software developed by IMFT [22]. Nieves-Remacha et al. [23] implemented this one fluid formulation for simulation of mass transfer in an industrial advanced flow reactor. A similar approach was developed by Marschall et al. [24] and was implemented in OpenFOAM [25, 26] for mass transfer in gas liquid bubble flow. In Nieves-Remacha [27] dissertation thesis, the two formulations of Haroun et al. [21] and Marschall et al. [24] were compared and found to be producing same steady state results for various simple test cases. Recently, Wang et al. [28] used this approach for simulating the gas liquid mass transfer in wetted wall column. They found the CFD results in reasonable agreement with the experimental values.

The aim of this work is to discuss the advantages and limitations of utilizing *one fluid formulation* for modeling the physical mass transfer of CO_2 in OpenFOAM CFD software. The one fluid formulation was implemented as an additional transport equation in the existing code of OpenFOAM CFD software and a separate procedure for reducing the overall computational time is proposed. The physical absorption of CO_2 was studied using N_2O analogy. A comparison of liquid side mass transfer coefficient value derived from the simulations with the standard theoretical correlation proposed by Higbie [29] is carried to study the aim. The investigations were carried for operating parameters such as flow rate, concentration of MEA and angle of inclination of plate. The simulation domain is two dimensional (2D) and the gas-liquid flow is counter current.

2 Modeling and analysis

2.1 Two phase flow modeling

The simulations are carried using "*interFoam*" module available as part of open source software OpenFOAM. The *interFoam* is based on color function volume of fluid method and is used in modeling incompressible two phase flows. The implementation involves description of each phase on fixed mesh using Eulerian approach, Eq. (1) and modeling interface using a color function. The color function used in OpenFOAM is volume fraction of secondary phase (α) and its value is derived by solving an additional transport, Eq. (2). The advection of volume fraction is modeled using multidimensional universal limiter with explicit solution (MULES) algorithm.

$$\rho \frac{\partial \vec{v}}{\partial t} + \vec{v}.\nabla \vec{v} = -\overrightarrow{\nabla P} + \rho \vec{g} + \mu \nabla^2 \vec{v} - F_{st} \tag{1}$$

$$\frac{\partial \alpha}{\partial t} + \nabla.\left(\vec{v}\alpha\right) = 0 \ . \tag{2}$$

By solving these equations , the values of velocity vector, and pressure and phase fraction values at each grid cell is derived at each time step. The cells fully occupied with secondary phase will have a value of $\alpha = 1$ and the cells fully occupied by primary phase will have value of $0 < \alpha < 1$ depending upon the flow conditions. The VOF approach involves solving of a single momentum equation for both the phases with volume averaged properties of at the interface defined by: density, Eq. (3) and viscosity, Eq. (4):

$$\rho = \rho_L \alpha_L + \rho_G \left(1 - \alpha_L\right) \tag{3}$$

$$\mu = \mu_L \alpha_L + \mu_G \left(1 - \alpha_L\right). \tag{4}$$

Where the subscripts "*L*" and "*G*" stands for liquid and gas phase respectively.

On similar lines, a single continuity Eq. (5) is solved for mass conservation:

$$\frac{\partial \rho}{\partial t} + \nabla.\left(\rho \vec{v}\right) = 0. \tag{5}$$

The last term in Eq. (1), F_{st} represent surface tension force and is modeled by using formulation proposed by Brackbill et al. [30], Eq. (6):

$$F_{st} = \frac{\sigma_{st} \rho k \nabla \alpha_L}{2\left(\rho_L + \rho_G\right)}. \tag{6}$$

Where σ_{st} is the surface tension coefficient; $\kappa = -\nabla.\vec{n}$ represents the surface curvature where $\vec{n}$ is unit interface normal vector. This normal vector is given by Eq. (7):

$$\vec{n} = \frac{\nabla \alpha}{\left|\nabla \alpha\right|}. \tag{7}$$

This normal vector is corrected at the wall boundaries to consider the effect of wall adhesion by relating with the liquid contact angle by Eq. (8):

$$\vec{n} = \vec{n}_w \cos\left(\theta_w\right) + \vec{t}_w \sin\left(\theta_w\right). \tag{8}$$

Where $\vec{n}_w$ and $\vec{t}_w$ are the normal and tangential vectors to the wall and θ_w is the contact angle between liquid and wall.

In *interFoam* formulation an additional interface compression term is added to the Eq. (2) in order to reduce the numerical diffusion at the interface and to have a sharp interface between the two immiscible phases. The modified Eq. (2) is given by Eq. (9):

$$\frac{\partial \alpha}{\partial t} + \nabla.\left(\vec{v}\alpha\right) + \nabla.\left(\vec{v}_r\left(\alpha\left(1-\alpha\right)\right)\right) = 0 \tag{9}$$

where $\vec{v}_r$ is the relative velocity between the phases. The modeling of this additional term and also the impact of various input values to this additional term can be found in detail in Deshpande et al. [31].

2.2 Mass transfer modeling

The one fluid formulation developed by Haroun et al. [21] was implemented for modeling the mass transfer between immiscible phases. This formulation involves modeling the effect of thermodynamic properties like diffusion and solubility within a scalar transport equation instead of using values derived from correlations. The modified additional equation for the specie transport using this approach is given by Eq. (10):

$$\frac{\partial C}{\partial t} + \nabla.\left(\vec{v}C - D\nabla C - \Phi\right) = 0. \tag{10}$$

The one fluid formulation solves a single transport, Eq. (10) for specie concentration across the two phases by treating the concentration as a function of phase fraction. The VOF involves the same approach for defining the flow properties like density and viscosity. The effect of concentration jump at the interface is included using the additional mass flux term Φ. This additional mass flux is due to the solubility of gaseous specie into the liquid and thus can be calculated using Henry's law. The flux term Φ modeled to include the solubility is given by the Eq. (11):

$$\Phi = -D\frac{C\left(1-H\right)}{\alpha_L + H\left(1-\alpha_L\right)}\nabla \alpha_L \tag{11}$$

where *D* stands for the effective diffusivity of the specie in the two-phase mixture. The *D* is calculated as a harmonic average of diffusion of specie in each phase and is given by Eq. (12):

$$D = \frac{D_L D_G}{\alpha_L D_G + \left(1-\alpha\right)_L D_L} \tag{12}$$

where the D_L and D_G represent the diffusion coefficient of specie in liquid and gas phase respectively. The *H* in Eq. (11) represent the dimensionless Henry's constant for the specie under consideration. It is defined as the ratio of concentration of specie in gas (C_G) to the concentration of specie in liquid (C_L) which is $H = C_G / C_L$. Note that the additional flux term Φ will have numerical values only at the interface and will be zero within the individual phases. This is because the $\nabla \alpha_L$ term in Eq. (11) is essentially zero in grid cells fully occupied by individual phase fraction.

3 Input parameters

The physical mass transfer of CO_2 was modeled using surrogate N_2O gas. This kind of approach was used in many studies involving physical mass transfer of CO_2 and is known as N_2O analogy. The N_2O analogy avoids the effect of reaction, between CO_2 and MEA, on absorption. An excellent review of using N_2O analogy in the context of CO_2 capturing analysis can be found in Monteiro and Svendsen [32]. The simulations were carried at isothermal conditions at a temperature of 298 K. The CO_2 loading on MEA solvent for current investigation was fixed at 20 %. It was chosen so that the current studies can be used as a preliminary work for reactive mass transfer. In reactive mass transfer, the value of CO_2 concentration dissolved in MEA will highly influence the equilibrium partial

pressure on the gas side of the interface and for CO_2 loading less than 30 % this influence was found negligible by Aronu et al. [33] and Wang et al. [28]. The solvent properties are chosen based on the concentration of MEA (% wt) which in our study vary between 10 to 40 %.

In the current simulation, pure N_2O gas was used on gas side. The gas density values were calculated using ideal gas law and viscosity values were taken from open literature for pure N_2O. The N_2O diffusivity within gas medium is taken equal to that of kinematic viscosity. The diffusivity value of N_2O in the solvent is calculated from correlation proposed by Versteeg and van Swaaij [34] as shown in Eq. (13).

$$D_{N_2O} = 5.07\times10^{-6}\exp\left(-\frac{2371}{T}\right)\left(\frac{\mu_{water}}{\mu_{soln}}\right)^{0.8} \quad (13)$$

where the μ_{water} and μ_{soln} are viscosities of pure water and carbonated solvents respectively. Properties like viscosity and density of carbonated solvents were taken from Weiland et al. [35] and surface tension values were taken from Fu et al. [36]. The Henry constant values were calculated from the Eq. (14)-(16) proposed by Penttilä et al. [37]. The units of Henry constant in their work is

$$H_{N_2O,water} = \exp\begin{pmatrix} 158.245-\dfrac{9048.596}{T} \\ -20.86.\ln(T)-0.00252.T \end{pmatrix} \text{ Pa.m}^3/\text{mol} \quad (14)$$

$$H_{N_2O,MEA} = -9172.5+39.598.T \quad \text{Pa.m}^3/\text{mol} \quad (15)$$

$$H_{N_2O,solvent} = H_{N_2O,water}.x_{water} + H_{N_2O,MEA}.x_{MEA} + A_1\left[x_{water}.x_{MEA}\right]\left[1-\frac{T}{A_2}\right]\exp\left[-A_3.x_{MEA}\right]. \quad (16)$$

Where in the Eq. (16) the A_1, A_2 and A_3 are constants with values of 3524641.533, 324.718 and 13.219 respectively. The x_{water} and x_{MEA} represent the mole fraction of water and MEA in the solvent. The calculated Henry constant values with units, as mentioned in Eq. (14), are then converted into dimensionless Henry constant by using Eq. (17)

$$H_{N_2O,dimless} = \frac{H_{N_2O,solvent}}{RT}. \quad (17)$$

Where R is the universal gas constant with value 8.314 $Pa.m^3.mole^{-1}.K^{-1}$ and T is temperature in K.

The contact angle value for solvent was taken as fixed at 40° as given in [28].

The ranges of values used in our simulations are as tabulated in Table 1. Units of all the variables used in the current simulations have SI units.

Table 1 Modeling input parameters

Parameter	Value/Range	Units
Operating temperature	298	K
MEA mass fraction	[0.1, 0.4]	g of MEA/g solvent
CO_2 loading	0.2	Mole of CO_2/ mol of MEA
Inlet N_2O mole fraction	1	Dimensionless
Liquid Reynolds number, Re_L	[83, 249]	Dimensionless
Gas Reynolds number, Re_G	200	Dimensionless
Henry coefficient	[1.42, 1.8]	Dimensionless
N_2O Diffusivity in solvent	[5E-10,9.98E-10]	m^2/s
Surface tension	0.0673	N/m
Solvent contact angle	40°	Degree
Gas Inlet concentration	40.896	$mole/m^3$

4 Geometry, mesh and boundary conditions

The current study was carried on 2D (two dimensional) geometry. The N_2O gas is the primary phase and the MEA solvent is the secondary phase and the flow was modeled by interFOAM. The geometry under simulation is shown in Fig. 1. The liquid enters the computational domain through a 1 mm inlet and leaves through a 1 mm outlet. The gas enters counter currently through a 4 mm inlet and leaves through a 4 mm outlet.

To avoid the gas phase entering the computational domain from the gas outlet, which is possible when the gas phase near the liquid inlet attains a higher relative velocity (because of high liquid velocity compared to gas) into

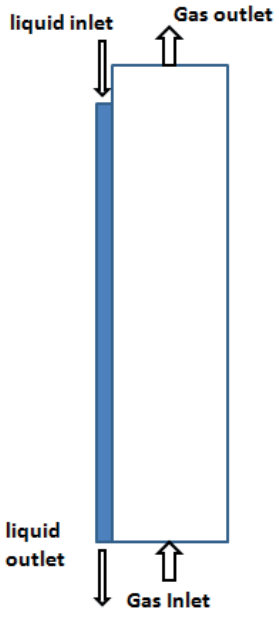

Fig. 1 Overall geometry under simulation

the domain, the gas chamber size in the current simulation was considered 10 % higher (55 mm) when compared to liquid plate height (50 mm).

Generic boundary conditions available in OpenFOAM were used in this simulation and are listed in Table 2. A comprehensive work for setting up a two dimensional investigation in OpenFOAM using generic boundary conditions can be found in [38], for further reading.

In their investigation of counter current gas liquid mass transfer Xu et al. [20] found that to capture the mass transfer effect with reasonable accuracy a mesh size of 0.07 *h*, where *h* is the film thickness, is required. Since the average film thickness in our study is 0.4 mm the minimum size of mesh required was 0.028 mm. But through our preliminary investigations to find the grid independency, we found that a mesh size of 0.00625 mm (approx. 0.015 *h*) is required in order to capture the mass transfer effectively. The requirement of higher mesh refinement can be due to the one fluid formulation used in our study which involves modeling of the very low diffusivity of gas in the liquid solvent. The lower diffusivity confines the gas concentration layer to regions near interface. A similar observation of high mesh refinement was made by Cooke [39]. In the remaining gas side geometry, a uniform mesh size of 0.0125 mm in the horizontal direction was used. Further refinement in this region wasn't affecting the final solution of concentration field, which can be due to the higher diffusivity of gas. In order to reduce the computational time, the size of 0.0125 mm was used in the gas side of domain. In the direction of height, a size of 0.1 mm was used. A snapshot of refined mesh is given in Fig. 2. The final mesh size was approximately 0.3 million hexahedra cells. The details of grid independency study can be found in the Appendix 1.

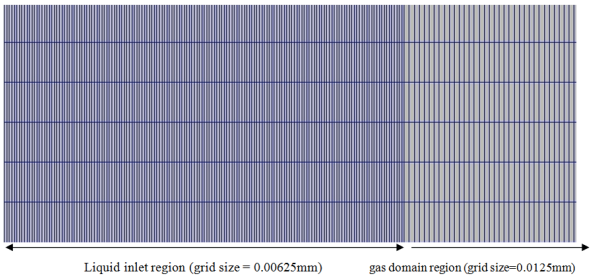

Fig. 2 Mesh size distribution in the domain

5 Solver setting and analysis of results

Higher order vanLeer scheme available in OpenFOAM was used to solve the continuity, momentum and concentration equations. The tolerance of 10^{-14} was used as convergence criteria. All the flow equations were solved transiently until steady state flow field was achieved. An adjustable time step was used with a maximum Courant number of 0.9. In order to reduce the simulation time, the flow field was solved initially on a coarse mesh with 0.028 mm in the film thickness region. Later this flow field was mapped on refined mesh with 0.00625 mm and further simulated transiently until steady state flow field was achieved. The concentration equation was then solved independently on the resulting flow field with a fixed time step of 10^{-5} s, until steady state was achieved. This procedure has resulted in reducing the overall computational time from several days to hours without compromising the "quality of the model", that is the final two phase flow field will be same as the flow field obtained by refined mesh. Note that this suggested procedure is suitable for problems involving steady state solutions and may not be suitable for obtaining transient solutions which are sensitive to initial conditions. Despite the suggested procedure to reduce the computation time, the time to obtain result for one flow condition that is from solving flow field on coarse mesh to solving concentration Eq. (10) was not less than 30 hours in total on a Dell workstation (DELL PRECISION T7810 (v2)) with 2 Intel Xeon E5-2630 v3 processors (16 core).

On obtaining the concentration values at steady state, the liquid side mass transfer coefficient is calculated from the simulation results using the Eq. (18)

$$k_L = F/\Delta C \tag{18}$$

Table 2 Boundary conditions

Boundary name	**U** (Velocity)	**p** (pressure)	**α** (phase fraction)	**C** (concentration)
Liquid inlet	surfaceNormalFixedValue	zeroGradient	FixedValue 1	zeroGradient
Liquid outlet	zeroGradient	zeroGradient	zeroGradient	zeroGradient
Gas inlet	surfaceNormalFixedValue	zeroGradient	FixedValue 0	FixedValue
Gas outlet	zeroGradient	totalPressure p0 0;	zeroGradient	zeroGradient
Wall on the liquid side	zeroGradient	zeroGradient	constantAlphaContactAngle θ = 40°	zeroGradient
Wall on the gas side	zeroGradient	zeroGradient	zeroGradient	zeroGradient

where F is the mass flux at the gas-liquid interface per unit area and ΔC is the difference between the concentration at the interface and bulk liquid. The results are compared with theoretical correlation proposed by Higbie [29] as Eq. (19)

$$k_L = 2\sqrt{\frac{D_L}{\pi\tau}}. \tag{19}$$

Where τ is the time of exposure calculated using an expression in Eq. (20) reported by Haroun et al. [40]:

$$\tau = L/|v_i|. \tag{20}$$

Where L is the length of the plate and v_i is the interfacial velocity.

The interfacial velocity is calculated using Nusselt [41] theory which is valid for laminar flows. The Nusselt expression (Eq. (21)) predicts the liquid velocity within the liquid film region as a function of distance from the plate surface. The expression also includes the effect of inclination of the plate with respect to the horizontal surface.

$$v = \frac{\rho_L g \delta^2 \sin(\beta)}{2\mu_L}\left[1-\left(\frac{z}{\delta}\right)^2\right]. \tag{21}$$

6 Results and discussion

6.1 Comparing the effect of flow rate

The counter current gas flow reduces and flattens the liquid surface velocity and the maximum liquid velocity can occur at a different position than that of interface. This kind of flow filed instabilities at micro scale near the interface can enhance the mass transfer by multitude, even in laminar flow conditions [42]. Hence a study of influence of liquid flow rate is of prime importance in understanding the mass transfer under counter current flow conditions. In this study, the effect of liquid flow rate on absorption of gas was studied at gas phase Reynolds number of Re_G = 200 and for liquid phase Reynolds number of 83 < Re_L < 249. This Re_G was the minimum value used in Yu et al. [42] experiments of counter current gas liquid absorption. Also, it was found in the Yu et al. [42] experiments that the gas phase velocity has little influence on the interface liquid velocity and hence the effect of varying gas phase velocity wasn't studied in our investigations. The liquid and gas Reynolds numbers are defined as:

$$Re_L = \frac{d_L u_L \rho_L}{\mu_L} \tag{22}$$

$$Re_G = \frac{d_G u_G \rho_G}{\mu_G}. \tag{23}$$

The liquid side mass transfer coefficient, k_L (with units mole / Pa.s.m^2) is calculated using Eq. (18) where the flux value F is calculated based on overall mass consumption at steady state. The mass conservation inherently states that the amount of N_2O dissolved through gas liquid interface is equal to the amount of N_2O removed by solvent at liquid outlet. This amount of N_2O removed at outlet when divided by interfacial area gives the mass flux value, F, in mole / m^2-s. The resulting liquid side mass transfer coefficient is then compared to Higbie [29] correlation for various Re_L and results are presented in Fig. 3.

The results agree very well with Higbie penetration theory at low Re_L and deviate at higher Re_L. The deviation at higher Re_L can be due to the influence of surface instabilities whose effects aren't included in the Higbie [29] model as mentioned in Yu et al. [42]. The surface instabilities will lead to deviation in the velocity from standard Nusselt [41] laminar profile. The deviations can be observed from the velocity profile of the liquid phase at the liquid outlet as presented in the Fig. 4(a)-(d).

Also, it can be due to the small size of geometry and parameters used from experimental data published in open literature. Since the current model is promising by accurately predicting the mass transfer coefficient values at low Re_L, it may be used by coupling with studies involving DNS to develop new correlations for higher Re_L and this will be part of our future work.

6.2 Comparing the influence of MEA concentration

Since at Re_L of 125 the Higbie [29] model was accurately approximating the liquid side mass transfer coefficient for solvent with MEA mass fraction of 30 %, as explained in the previous section, the current study was carried at Re_L of 125. The influence of MEA mass fraction in the liquid solvent on the liquid side mass transfer coefficient has

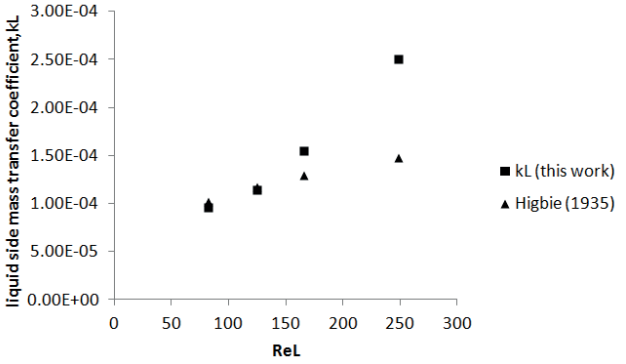

Fig. 3 Liquid side mass transfer coefficient is compared to Higbie [29] correlation for varying Re_L

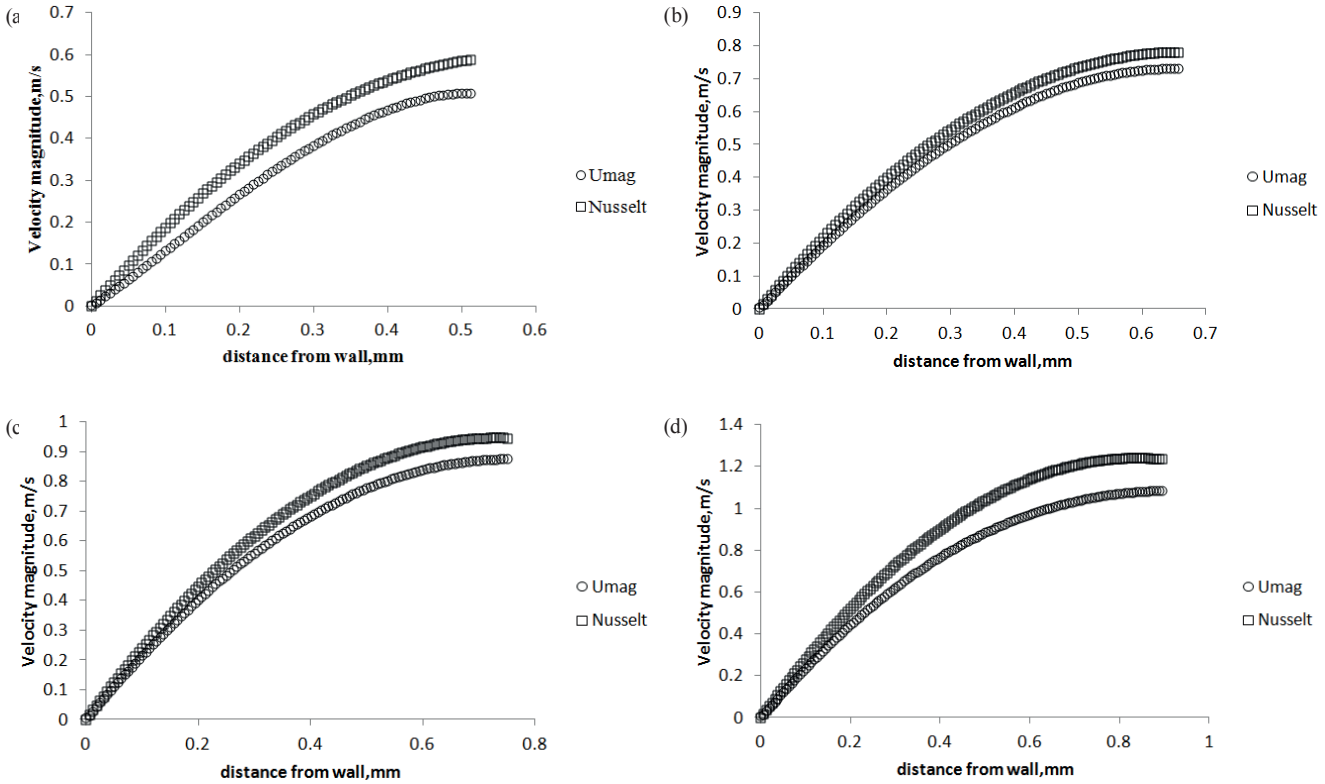

Fig. 4 Comparison of velocity profile with Nusselt [41] laminar profile (a) at Re_L = 83 at Re_G = 200; (b) at Re_L = 125 at Re_G = 200; (c) at Re_L = 166 at Re_G = 200; (d) at Re_L = 249 at Re_G = 200

been studied for four values of: 10 %, 20 %, 30 % and 40 % respectively. The results are as shown in Fig. 5.

For MEA mass fraction less than 30 % the Higbie [29] model over estimates and for mass fraction of 40 % underestimates the liquid side mass transfer coefficient. Also for MEA mass fraction of 30 % the Higbie [29] model accurately estimates the liquid side mass transfer coefficient. This kind of behavior was observed by Sebastia-Saez et al. [18]. Such variations occurs presumably due to the variation of liquid properties like kinematic viscosity

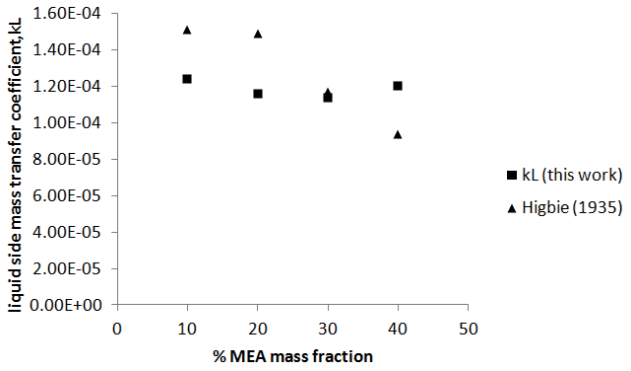

Fig. 5 Comparison of liquid side mass transfer coefficient obtained from this work with Higbie [29] for varying MEA concentration

and density of the solvent based on the MEA mass fraction. Hence it is safe to say that, using this approach a better estimate of physical mass transfer can be obtained than theoretical models. Since the MEA mass fraction is an important parameter influencing the chemical absorption rate [43] the current approach is suggested for estimating the enhancement factor and studies involving the design of CO_2 reactors.

6.3 Comparing the influence of angle of inclination of plate to the horizontal plane

In the two previous sections the film was flowing downward on a vertical plate. But in practice corrugated sheets are used for designing packed beds. These packed beds are generally made of metal sheets of steel and have corrugated textures with an angle of 45° or 60° between the corrugations respectively [13]. In this study, the influence of the plate inclination on the liquid side mass transfer coefficient was also investigated for inclinations of 45° and 60° at Re_L of 83 for solvent with MEA mass fraction of 30 %. Fig. 6 shows simulation domain of an inclined plate in our simulation. The results are shown in Fig. 7. The liquid side mass transfer coefficient is exactly approximated by

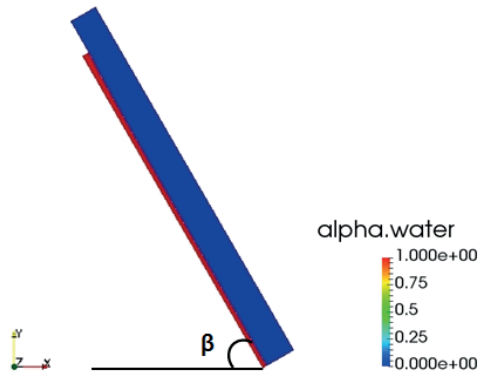

Fig.6 Domain inclined to the horizontal plane by an angle of β

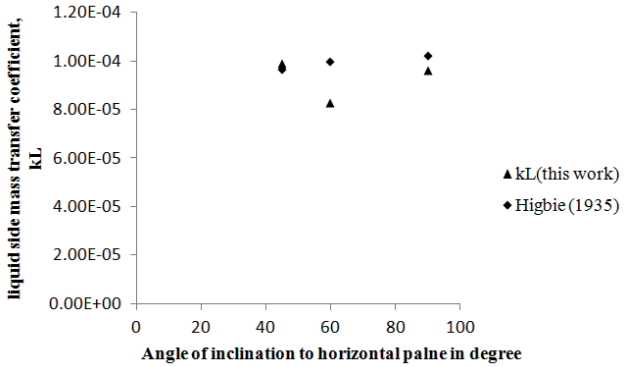

Fig. 7 Comparison of liquid side mass transfer coefficient obtained from this work with Higbie [29] at different inclinations of flat plate

Higbie [29] model. Hence it is concluded that the current model allows the modeling of physical mass transfer in counter current flow on corrugated sheets, which are used to increase the available surface area per unit volume of the packed bed, accurately.

7 Conclusions

In this study we implement and analyze the advantages and limitations of one fluid formulation approach for CO_2 physical mass transfer into MEA. The domain considered is a flat plate and gas liquid flow is counter current. The analysis was carried for operating parameters like liquid phase Reynolds number in the range of $83 < Re_L < 249$, MEA mass fraction in the range of 0.1 to 0.4 and for the angle of inclination of flat plate varying between 45° to 90° respectively.

The results clearly show that the model effectively captures the deviation in liquid side mass transfer coefficient due to the surface instabilities which are significant at higher Reynolds numbers. The effect of liquid properties which vary with the mass fraction of MEA in the solvent are also predicted with greater accuracy. These effects are generally neglected in the standard correlations. The model also shows that the standard Higbie correlation is well suitable for modeling the flows at low Reynolds number.

The grid independent studies show that a size of 6.25 µm is required in the interface region for effectively using this approach. The requirement of this high mesh resolution results in high computational resource time. In order to reduce the overall computational time we adopted a sequential procedure of solving the concentration equation independently on the desired flow field. Also the time required for obtaining the flow field was further reduced by first solving the flow field on a coarse mesh and mapping the result on refined a mesh. This procedure was found to reduce the overall computational time from days to hours. However it should be noted that the suggested procedure is suitable for problems involving steady state solutions and may not be suitable for obtaining transient solutions which are highly dependent on initial conditions.

In conclusion, it can be said that the CFD modeling of mass transfer by one fluid formulation is proven to be a promising approach and an alternative to experimentation. The higher accuracy of this approach is due to the consideration of the effect of thermodynamic properties like diffusion and solubility on mass transfer coefficient instead of using derived values from correlations. Hence future CFD investigations of micro structure impact on CO_2 mass transfer can be carried using this approach and our suggested procedure can be adopted for reducing the simulation time effectively.

Acknowledgement

This study was financially supported by the Anadolu University Research Fund (Project No: 1603F123).

Nomenclature

Latin symbols

C	concentration (mole/m^3)
D	mass diffusivity (m^2/s)
d	hydraulic diameter (m)
F	mass flux (mole/m^2-s)
g	acceleration of gravity (m/s^2)
H	henry constant (-)
h	film thickness (mm)
k	liquid side mass transfer coefficient (mole/Pa.s.m^2)
L	length of the flat plate (m)
R	universal gas constant (Pa.m^3.mole^{-1}.K^{-1})
T	temperature (K)
v	velocity (m/s)

x	mole fraction in solvent
z	distance of grid cell from wall (m)

Greek symbols

α	volume fraction(-)
ρ	density (kg/m^3)
μ	viscosity (Pa s)
β	plate inclination angle (-)
θ	contact angle between liquid and solid wall (-)
τ	time of exposure (s)
κ	surface curvature (m^{-1})
σ	surface tension coefficient (Nm^{-1})
δ	liquid film thickness (m)
Φ	(mass) flux term (kg/m$^{2\text{-}s}$)

Subscripts

G	gas phase
L	liquid phase
st	surface tension
w	wall
i	interface

Dimensionless numbers

Re	Reynolds number

Vectors

$\vec{n}$	normal vector (dimensionless)
$\vec{n}_w$	normal vector to the wall (dimensionless)
$\vec{t}_w$	tangential vector to the wall (dimensionless)
$\vec{v}_r$	relative velocity between the phases (m/s)

Appendix 1

The grid independence study was aimed to find out the minimum number of nodes after which an increase in the number of nodes wouldn't affect the concentration measured at the outlet significantly. The study was carried for MEA weight percentage of 30 %, at Re_L of 125 and Re_G of 200. The resulting graph, Appendix 1, of liquid outlet concentration as a function of number of nodes clearly shows that a number of 160 nodes (6.25 μm) in the liquid inlet region of 1 mm are sufficient to capture the outlet concentration.

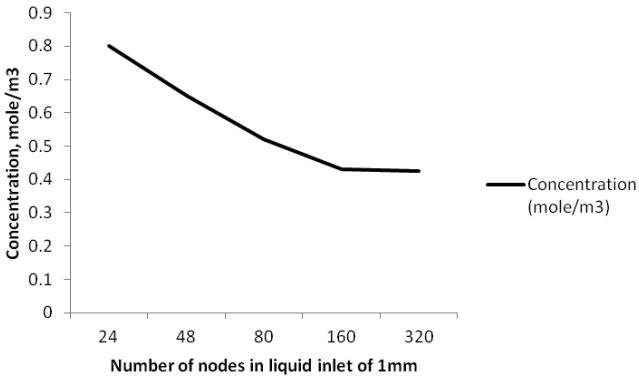

Appendix 1 Concentration at liquid outlet as a function of number of nodes in liquid inlet

References

[1] Aaron, D., Tsouris, C. "Separation of CO_2 from Flue Gas: A Review", Separation Science and Technology, 40(1–3), pp. 321–348, 2005. https://doi.org/10.1081/SS-200042244

[2] Rezakazemi, M., Sadrzadeh, M., Matsuura, T. "Thermally stable polymers for advanced high-performance gas separation membranes", Progress in Energy and Combustion Science, 66, pp. 1–41, 2018. https://doi.org/10.1016/j.pecs.2017.11.002

[3] Webley, P. A. "Adsorption technology for CO_2 separation and capture: a perspective", Adsorption, 20(2–3), pp. 225–231, 2014. https://doi.org/10.1007/s10450-014-9603-2

[4] Mesbah, M., Shahsavari, S., Soroush, E., Rahaei, N., Rezakazemi, M. "Accurate prediction of miscibility of CO_2 and supercritical CO_2 in ionic liquids using machine learning", Journal of CO2 Utilization, 25, pp. 99–107, 2018. https://doi.org/10.1016/j.jcou.2018.03.004

[5] Shirazian, S., Marjani, A., Rezakazemi, M. "Separation of CO_2 by single and mixed aqueous amine solvents in membrane contactors: fluid flow and mass transfer modeling", Engineering with Computers, 28(2), pp. 189–198. 2012. https://doi.org/10.1007/s00366-011-0237-7

[6] Luis, P. "Use of monoethanolamine (MEA) for CO_2 capture in a global scenario: Consequences and alternatives", Desalination, 380, pp. 93–99, 2016. https://doi.org/10.1016/j.desal.2015.08.004

[7] Rezakazemi, M., Heydari, I., Zhang, Z. "Hybrid systems: Combining membrane and absorption technologies leads to more efficient acid gases (CO_2 and H_2S) removal from natural gas", Journal of CO2 Utilization, 18, pp. 362–369, 2017. https://doi.org/10.1016/j.jcou.2017.02.006

[8] Stéphenne, K. "Start-up of World's First Commercial Post-combustion Coal Fired CCS Project: Contribution of Shell Cansolv to SaskPower Boundary Dam ICCS Project", Energy Procedia, 63, pp. 6106–6110, 2014. https://doi.org/10.1016/j.egypro.2014.11.642

[9] Pham, D. A., Lim, Y.-I., Jee, H., Ahn, E., Jung, Y. "Porous media Eulerian computational fluid dynamics (CFD) model of amine absorber with structured-packing for CO_2 removal", Chemical Engineering Science, 132, pp. 259–270, 2015. https://doi.org/10.1016/j.ces.2015.04.009

[10] Li, W., Zhao, X., Liu, B., Tang, Z. "Mass Transfer Coefficients for CO_2 Absorption into Aqueous Ammonia Using Structured Packing", Industrial & Engineering Chemistry Research, 53(14), pp. 6185–6196, 2014. https://doi.org/10.1021/ie403097h

[11] Aroonwilas, A., Chakma, A., Tontiwachwuthikul, P., Veawab, A. "Mathematical modelling of mass-transfer and hydrodynamics in CO_2 absorbers packed with structured packings", Chemical Engineering Science, 58(17), pp. 4037–4053, 2003. https://doi.org/10.1016/S0009-2509(03)00315-4

[12] Aroonwilas, A., Tontiwachwuthikul, P., Chakma, A. "Effects of operating and design parameters on CO_2 absorption in columns with structured packings", Separation and Purification Technology, 24(3), pp. 403–411, 2001. https://doi.org/10.1016/S1383-5866(01)00140-X

[13] Kohrt, M., Ausner, I., Wozny, G., Repke, J.-U. "Texture influence on liquid-side mass transfer", Chemical Engineering Research and Design, 89(8), pp. 1405–1413, 2011. https://doi.org/10.1016/j.cherd.2011.01.010

[14] Fischer, L., Bühlmann, U., Melcher, R. "Characterization of High-Performance Structured Packing", Chemical Engineering Research and Design, 81(1), pp. 79–84, 2003. https://doi.org/10.1205/026387603321158221

[15] Sebastia-Saez, D., Gu, S., Ranganathan, P., Papadikis, K. "3D modeling of hydrodynamics and physical mass transfer characteristics of liquid film flows in structured packing elements", International Journal of Greenhouse Gas Control, 19, pp. 492–502, 2013. https://doi.org/10.1016/j.ijggc.2013.10.013

[16] Haroun, Y., Raynal, L. "Use of Computational Fluid Dynamics for Absorption Packed Column Design", Oil and Gas Science and Technology, 71(3), pp. 1–18, 2016. https://doi.org/10.2516/ogst/2015027

[17] Hoffmann, A., Ausner, I., Repke, J.-U., Wozny, G. "Fluid dynamics in multiphase distillation processes in packed towers", Computer Aided Chemical Engineering, 18, pp. 199–204, 2004. https://doi.org/10.1016/S1570-7946(04)80099-3

[18] Sebastia-Saez, D., Gu, S., Ranganathan, P., Papadikis, K. "Micro-scale CFD modeling of reactive mass transfer in falling liquid films within structured packing materials", International Journal of Greenhouse Gas Control, 33, pp. 40–50, 2015. https://doi.org/10.1016/j.ijggc.2014.11.019

[19] Sebastia-Saez, D., Gu, S., Ranganathan, P., Papadikis, K. "Micro-scale CFD study about the influence of operative parameters on physical mass transfer within structured packing elements", International Journal of Greenhouse Gas Control, 28, pp. 180–188, 2014. https://doi.org/10.1016/j.ijggc.2014.06.029

[20] Xu, Y. Y., Paschke, S., Repke, J.-U., Yuan, J. Q., Wozny, G. "Computational Approach to Characterize the Mass Transfer between the Counter-Current Gas-Liquid Flow", Chemical Engineering & Technology, 32(8), pp. 1227–1235, 2009. https://doi.org/10.1002/ceat.200900099

[21] Haroun, Y., Legendre, D., Raynal, L. "Volume of fluid method for interfacial reactive mass transfer: Application to stable liquid film", Chemical Engineering Science, 65(10), pp. 2896–2909, 2010. https://doi.org/10.1016/j.ces.2010.01.012

[22] Legendre, D., Magnaudet, J. "The lift force on a spherical bubble in a viscous linear shear flow", Journal of Fluid Mechanics, 368, pp. 81–126, 1998. https://doi.org/10.1017/S0022112098001621

[23] Nieves-Remacha, M. J., Kulkarni, A. A., Jensen, K. F. "OpenFOAM Computational Fluid Dynamic Simulations of Single-Phase Flows in an Advanced-Flow Reactor", Industrial and Engineering Chemistry Research, 54(30), pp. 7543–7553, 2015. https://doi.org/10.1021/acs.iecr.5b00232

[24] Marschall, H., Hinterberger, K., Schüler, C., Habla, F., Hinrichsen, O. "Numerical simulation of species transfer across fluid interfaces in free-surface flows using OpenFOAM", Chemical Engineering Science, 78, pp. 111–127, 2012. https://doi.org/10.1016/j.ces.2012.02.034

[25] Jasak, H., Weller, H. G. "Interface Tracking Capabilities of the Inter-Gamma Differencing Scheme", [pdf] Publisher Unknown, pp. 1–9, 1995. Availabe at: http://powerlab.fsb.hr/ped/kturbo/OpenFOAM/docs/InterTrack.pdf [Accessed: 23 February 1995]

[26] Rusche, H. "Computational Fluid Dynamics of Dispersed Two-Phase Flows at High Phase Fractions", PhD Thesis, Imperial College of Science, Technology & Medicine, 2002. [online] Availabe at: http://powerlab.fsb.hr/ped/kturbo/OpenFOAM/docs/HenrikRuschePhD2002.pdf [Accessed: 01 December 2002]

[27] Nieves-Remacha, M. J. "Microreactor Technology: Scale-up of Multiphase Continuous Flow Chemistries", PhD Thesis, Massachusetts Institute of Technology, 2014. [online] Availabe at: http://hdl.handle.net/1721.1/91068 [Accessed: 30 June 2014]

[28] Wang, C., Xu, Z., Lai, C., Whyatt, G., Marcy, P., Sun, X. "Hierarchical calibration and validation for modeling bench-scale solvent-based carbon capture. Part 1: Non-reactive physical mass transfer across the wetted wall column", Greenhouse Gases: Science and Technology, 7(4), pp. 706–720, 2017. https://doi.org/10.1002/ghg.1682

[29] Higbie, R. "The Rate of Absorption of a Pure Gas Into a Still Liquid During Short Periods of Exposure", Transactions of American Institute of Chemical Engineers, 31(2), pp. 365–389, 1935.

[30] Brackbill, J. U., Kothe, D. B., Zemach, C. "A continuum method for modeling surface tension", Journal of Computational Physics, 100(2), pp. 335–354, 1992. https://doi.org/10.1016/0021-9991(92)90240-Y

[31] Deshpande, S. S., Anumolu, L., Trujillo, M. F. "Evaluating the performance of the two-phase flow solver interFoam", Computational Science & Discovery, 5(1), pp. 1–36, 2012. https://doi.org/10.1088/1749-4699/5/1/014016

[32] Monteiro, J. G. M.-S., Svendsen, H. F. "The N_2O analogy in the CO_2 capture context: Literature review and thermodynamic modelling considerations", Chemical Engineering Science, 126, pp. 455–470, 2015. https://doi.org/10.1016/j.ces.2014.12.026

[33] Aronu, U. E., Gondal, S., Hessen, E. T., Haug-Warberg, T., Hartono, A., Hoff, K. A., Svendsen, H. F. "Solubility of CO_2 in 15, 30, 45 and 60 mass% MEA from 40 to 120 °C and model representation using the extended UNIQUAC framework", Chemical Engineering Science, 66(24), pp. 6393–6406, 2011. https://doi.org/10.1016/j.ces.2011.08.042

[34] Versteeg, G. F., van Swaaij, W. P. M. "Solubility and Diffusivity of Acid Gases (CO_2, N_2O) in Aqueous Alkanolamine Solutions", Journal of Chemical and Engineering Data, 33(1), pp. 29–34, 1988. https://doi.org/10.1021/je00051a011

[35] Weiland, R. H., Dingman, J. C., Cronin, D. B., Browning, G. J. "Density and Viscosity of Some Partially Carbonated Aqueous Alkanolamine Solutions and Their Blends", Journal of Chemical and Engineering Data, 43(3), pp. 378–382, 1998. https://doi.org/10.1021/je9702044

[36] Fu, D., Xu, Y., Wang, L., Chen, L. "Experiments and model for the surface tension of carbonated monoethanolamine aqueous solutions", Science China Chemistry, 55(7), pp. 1467–1473, 2012. https://doi.org/10.1007/s11426-012-4641-7

[37] Penttilä, A., Dell'Era, C., Uusi-Kyyny, P., Alopaeus, V. "The Henry's law constant of N_2O and CO_2 in aqueous binary and ternary amine solutions (MEA, DEA, DIPA, MDEA, and AMP)", Fluid Phase Equilibria, 311, pp. 59–66, 2011. https://doi.org/10.1016/j.fluid.2011.08.019

[38] Tong, Z., Marek, A., Hong, W., Repke, J.-U. "Experimental and Numerical Investigation on Gravity-Driven Film Flow over Triangular Corrugations", Industrial and Engineering Chemistry Research, 52(45), pp. 15946–15958, 2013. https://doi.org/10.1021/ie303038c

[39] Cooke, J. J. "Modelling of reactive absorption in gas-liquid flows on structured packing", PhD Thesis, University of Southampton, 2016.

[40] Haroun, Y., Raynal, L., Legendre, D. "Mass transfer and liquid hold-up determination in structured packing by CFD", Chemical Engineering Science, 75, pp. 342–348, 2012. https://doi.org/10.1016/j.ces.2012.03.011

[41] Nusselt, W. "Die Oberflächenkondensation des Wasserdampfes", (The surface condensation of water vapor), ZEITSCHRIFT DES VEREINES DEUTSCHER INGENIEURE, 60, pp. 541–546, 1916. (in German)

[42] Yu, L.-M., Zeng, A.-W., Yu, K. T. "Effect of Interfacial Velocity Fluctuations on the Enhancement of the Mass-Transfer Process in Falling-Film Flow", Industrial and Engineering Chemistry Research, 45(3), pp. 1201–1210. 2006. https://doi.org/10.1021/ie050855q

[43] Meldon, J. H., Morales-Cabrera, M. A. "Analysis of carbon dioxide absorption in and stripping from aqueous monoethanolamine", Chemical Engineering Journal, 171(3), pp. 753–759, 2011. https://doi.org/10.1016/j.cej.2011.05.099